sions, 1969 (MIT Press, Cambridge, Mass., 1969), p. 1051.

[9]A. Dalgarno and A. E. Kingston, Proc. Roy. Soc. (London) 73, 455 (1959).

[10]R. E. Olson, F. T. Smith, and E. Bauer, Appl. Opt. 10, 1848 (1971).

[11]C. Bottcher and M. Oppenheimer, J. Phys. B 5, 492 (1972).

[12]R. E. Olson, Phys. Rev. A 2, 121 (1970).

[13]M. Barat and W. Lichten, Phys. Rev. A 6, 211 (1972).

[14]W. L. McMillan, Phys. Rev. A 4, 69 (1971).

[15]As a note of proof, Melius and Goddard have investigated the effect of the Σ-Π crossing in the $Li^+ + Na$ reaction and also arrive at this same conclusion, C. F. Melius and W. A. Goddard III (private communication).

[16]J. Perel and A. Y. Yahiku, *Fifth International Conference on the Physics of Electronic and Atomic Collisions, Leningrad*, 1967 (Nauka, Leningrad, 1967), p. 400.

[17]C. F. Melius (private communication).

[18]D. Rapp and W. E. Francis, J. Chem. Phys. 37, 2631 (1962).

[19]G. F. Drukarev, *Fifth International Conference on the Physics of Electronic and Atomic Collisions, Leningrad*, 1967 (Nauka, Leningrad, 1967), p. 10.

[20]H. Rosenthal and H. M. Foley, Phys. Rev. Letters 23, 1480 (1969).

PHYSICAL REVIEW A VOLUME 6, NUMBER 5 NOVEMBER 1972

Ionization Cross Sections for H_2, N_2, and CO_2 Clusters by Electron Impact

Franco Bottiglioni, Jacques Coutant, and Mario Fois
Association Euratom-CEA Département de la Physique du Plasma et de la Fusion Contrôlée, Centre d'Etudes Nucléaires, Boîte Postale n°6, 92 Fontenay-aux-Roses, France
(Received 29 March 1972)

Clusters of condensed matter which are produced under some particular conditions in supersonic molecular jets can be ionized by electrons. Measured ionization cross sections show a sharp dependence on N, the mean number of molecules per cluster. For small clusters ($\bar{N} < 50$) the cross sections increase as N; for larger clusters as about $\bar{N}^{2/3}$. Furthermore the electron initial energy W_{eM}, for which the cross section is maximum, increases with N. In this paper we present a model for the computation of the cluster ionization cross sections which includes the energy losses inside the cluster of both primary and secondary electrons. The escape probability for secondary electrons is given as a function of their initial position and energy. This latter is related to the primary-electron energy. Results of these computations for H_2, CO_2, and N_2 clusters are in good agreement with experimental data.

I. INTRODUCTION

The formation of molecular clusters in free-expansion supersonic jets has been observed by Becker *et al.*[1] For gases such as CO_2, cluster formation occurs above a critical pressure even at room temperature. Permanent gases such as N_2 or H_2, on the contrary, must be near their liquefaction temperature before expansion in order to form clusters.

As shown by Raoult, Farges, and Rouault[2] and by Audit[3] these clusters have a crystalline structure, and their size is determined by the expansion parameters: pressure ratio, nozzle-skimmer distance, nozzle shape and size. Clusters are ionized (positive charge) by electron collisions[4-9] and can be accelerated up to high energies in electrostatic accelerators.[4-7]

The ionization cross section we are concerned with in this paper has to be defined. Because of ionization, the attenuation of a neutral cluster beam with intensity I_0 and velocity v_c, each cluster containing N molecules, which intersects an electron target, length dl, electron density n_e, electron velocity $v_e \gg v_c$, can be written as

$$dI_0 = -I_0 \sigma n_e (v_e/v_c) dl \ , \qquad (1.1)$$

where $\sigma(N, W_{e0})$ is the cluster ionization cross section and W_{e0} is the electron energy.

Measurements of σ are uneasy due to the spread in the cluster masses. Generally it is possible to measure the mean molecular mass number $\bar{N}$ of the cluster beam, without knowing $f(N)$, the distribution function of the cluster mass. The experimental cross section is related to $\bar{N}$. Therefore $\sigma_{expt}(\bar{N}, W_{e0})$ defined as in (1.1) is actually

$$\sigma_{expt}(\bar{N}, W_{e0}) = \sigma_{av}(N, W_{e0}) = \sum_{1}^{N_{max}} f(N)\sigma(N, W_{e0}) \Big/ \sum_{1}^{N_{max}} f(N) \ . \qquad (1.2)$$

Ionization cross sections for hydrogen clusters under electron impact have been measured by Tay[7]; for argon and CO_2 clusters by Falter *et al.*[8] These cross sections are measured at a given electron energy as a function of the mean value of the number of molecules per cluster.

The most important features of their results are the following: (a) At constant energy, the cross section is proportional to the mean mass number of the cluster $\bar{N}$ up to a critical value, roughly

equal to 50 molecules per cluster; above this value, it increases as about $\bar{N}^{2/3}$. (b) At constant mean mass number, the cross section versus electron energy exhibits a maximum; the electron energy W_{eM} for which this maximum occurs is greater than the corresponding value for the molecular cross section and increases with $\bar{N}$.

Qualitatively, the first feature is interpreted as follows: The cluster ionization cross section is the product of two terms. The first one, proportional to $N^{2/3}$, is the geometrical cross section of a cluster containing N molecules and supposed to be spherical. The second one is the probability for an electron colliding with the cluster to make at least one ionizing collision inside it. This term is equal to $1-e^{-l/\lambda}$. The mean distance l traveled by an electron inside the cluster is proportional to $N^{1/3}$; λ, the ionization mean free path of an electron in the solid, is constant at constant electron energy.

For low values of N, $1-e^{-l/\lambda}$ is nearly equal to l/λ, that is, proportional to $N^{1/3}$, so that the ionization cross section increases as N; for high values of N, on the contrary, $1-e^{-l/\lambda}$ becomes equal to unity so that the cross section increases as $N^{2/3}$. No satisfactory explanation has been given for the second feature. We have improved this qualitative picture by taking into account the electron energy losses inside a cluster. Because of these losses, the average energy of an electron passing through a cluster is lower than its initial energy. Therefore, the maximum of the cluster ionization cross section will occur for an initial electron energy W_{eM} which increases with the cluster mass number N. Furthermore, the secondary electron, created by ionization, loses its energy and will escape only if it reaches the cluster surface with enough energy. It is possible to calculate an escape probability for the secondary electron which depends (i) on the position where the ionization occurs, (ii) on the cluster size, (iii) on the initial energy of the secondary electron, and (iv) on the scattering undergone on the cluster molecules. After computing the primary-electron losses and the secondary-electron escape probability, it is possible, by integrating over each primary-electron path and over all possible electron trajectories, to compute, for a given set of N and of the initial electron energy W_{e0}, the cluster ionization cross section $\sigma(N, W_{e0})$.

These calculations are undertaken in this paper. We shall first describe the cross-section computation scheme in Sec. II, then we shall investigate the electron collision processes in order to compute the primary-electron energy losses and the secondary-electron recombination probability, which both affect the cluster ionization cross section [Eq. (2.11)]. The electron energy losses will be examined in Sec. III, electron scattering inside clusters in Sec. IV, and the relation between primary- and secondary-electron energies in Sec. V. Section VI is devoted to the electron-range calculation, the computation results are discussed and compared with experimental data in Sec. VII, and some concluding remarks are presented in Sec. VIII. The rationalized mksa system is used, but energies are in electron volts.

II. CALCULATION OF CLUSTER IONIZATION CROSS SECTION

In this paper we have calculated both $\sigma_{expt}(\bar{N}, W_{e0})$ as defined in Eq. (1.2) in the case of a Poisson distribution

$$f(K) = e^{-\bar{K}} \bar{K}^K / K!\,,$$

with

$$K = \bar{K} N/\bar{N} \quad (\bar{K} = 5 \text{ or } 10) \quad (K = 1, 2, \ldots, n)$$

and $\sigma(N, W_{e0})$, that is, for a cluster with a fixed mass number. The difference between these two values is never significant when $N = \bar{N}$, so we consider single-mass clusters only.

We first assume that clusters are spherical; their geometrical cross section is therefore

$$s = \pi R_c^2 = \pi (3NM/4\pi\rho)^{2/3}\,, \tag{2.1}$$

where R_c is the cluster radius, ρ is the specific mass of the considered solid, and M is the mass of the corresponding molecule. The assumption of sphericity is of course very idealistic; nevertheless, hydrogen, nitrogen, and CO_2 belong to the cubic system, and the geometrical cross section must increase as R_c^2 even if the numerical factor is somewhat different.

Let us now consider (see Fig. 1) an electron with energy W_e impinging at point A on a spherical cluster. The distance h between the electron trajectory and the cluster center is called "cluster impact parameter." The number of ionizing collisions made by an electron between B and B', i.e., after a path inside the cluster between x and $x+dx$, is

$$dn = \sigma(1,\ W_e(x)) n_0 F(W_{s0}(x),\ x)\, dx\,. \tag{2.2}$$

Therefore, the probability for the electron to make at least one effective ionizing collision is

$$p(h) = 1 - \exp\Big[-n_0 \int_0^{2(R_c^2 - h^2)^{1/2}} \sigma(1,\ W_e(x)) \times F(W_{s0}(x),\ x)\, dx \Big]\,. \tag{2.3}$$

The meaning of quantities appearing in the two preceding equations is as follows:

$$W_e(x) = W_{e0} - \int_0^x \left(\frac{dW_e}{ds}\right) ds\,; \tag{2.4}$$

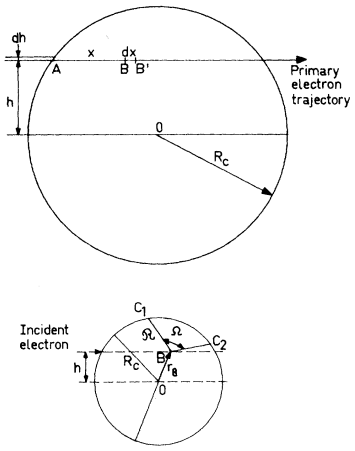

FIG. 1. Collision of an electron with a cluster at a "cluster impact parameter" h.

dW_e/ds is the electron energy loss per unit path length, $\sigma(1, W_e)$ is the molecular ionization cross section by electron impact, and $n_0 = \rho/M$ is the molecular density of the crystal.

The term $F(W_{s0}(x), x)$ is the probability for a secondary electron produced by ionization of a molecule at x with an initial energy $W_{s0}(x)$ to escape out of the cluster. As shown in Sec. III, $W_{s0}(x)$ is related to $W_e(x)$; to $W_{s0}(x)$ corresponds a value of the range $\mathcal{R}$ which is the maximum distance from its origin the secondary electron can travel before losing, in its random walk, enough energy to be stopped. The secondary electron can escape only if the vector of its stopping point is located inside the cone $C_1\hat{B}C_2$, the solid angle Ω of which (Fig. 1) is a function of r_B, R_0, and $\mathcal{R}$. Hence, the escaping probability $F(W_{s0}(x), x)$ is $\Omega/4\pi$ since the mean direction of motion is isotropically distributed. If we write the dimensionless parameters

$$U = r_B/R_c\,, \quad v = \mathcal{R}/R_c\,,$$

where r_B is the radial vector corresponding to x (Fig. 1) it can be easily shown that

$$F(U, v) = [(U+v)^2 - 1]/4Uv\,. \tag{2.5}$$

F depends on W_{s0} through the range $\mathcal{R}$.

We can now express the cluster beam attenuation through two consecutive independent processes: (a) cluster collisions with electrons in a target with length dl and density n_e, the corresponding probability being

$$p_1(l)\,dl = \pi R_c^2 n_e (v_e/v_c)\,dl\,; \tag{2.6}$$

(b) ionization inside the cluster by primary electrons colliding with "cluster impact parameter" h, without recombination of secondary electrons, the corresponding probability being

$$p_2(h)\,dh = \frac{2h}{R_c^2}\left\{1 - \exp\left[-n_0\int_0^{2(R_c^2-h^2)^{1/2}} \sigma(1, W_e(x)) \times F(W_{s0}(x), x)dx\right]\right\}dh\,, \tag{2.7}$$

that is, the probability for a collision between h and $h+dh$,

$$p_3(h)\,dh = 2\pi h\,dh/\pi R_c^2\,, \tag{2.8}$$

multiplied by the probability for the electron to make at least one effective ionizing collision, given by Eq. (2.3). Therefore the number of clusters effectively ionized in passing through an electron target of thickness dl is

$$dI = -I_0 p_1(l)\,dl \int_0^{R_c} p_2(h)\,dh\,. \tag{2.9}$$

Integration of Eq. (2.9) over a target thickness l yields the cluster beam attenuation

$$I/I_0 = \exp\left(-\pi R_c^2 n_e \frac{V_e}{V_c} l \int_0^{R_c} \frac{2h}{R_c^2}\left\{1 - \exp\left[-n_0\int_0^{2(R_c^2-h^2)^{1/2}} \sigma(1, W_e(x))\,F(W_{s0}(x), x)\,dx\right]\right\}dh\right) \tag{2.10}$$

and comparison with Eq. (1.1) gives the required cross section

$$\sigma(N, W_{e0}) = 2\pi \int_0^{R_c} h\{1 - \exp\,[-n_0 \int_0^{2(R_c^2-h^2)^{1/2}} \sigma_0(1, W_e(x))\,F(W_{s0}(x), x)dx]\}\,dh\,. \tag{2.11}$$

III. ENERGY LOSS OF ELECTRONS INSIDE CLUSTERS

A. High Energy

The collisional energy loss per unit path length for electrons passing through matter is given by Bethe's formula,[10] in the limit of validity of the first Born approximation. For energies smaller than the electron rest energy, the density effect and the relativistic corrections are negligible as are the radiation losses. Hence the total energy loss can be written as follows:

$$\frac{dW_e}{ds} \simeq -\frac{a_1 z}{W_e}\ln\left(\frac{a_2 W_e}{z}\right) \text{eV m}^{-1}\,, \tag{3.1}$$

where $a_1 = K_1 q^2 n/8\pi\epsilon_0^2$, W_e is the electron energy, n is the atomic density of the cluster, $K_1 = \sigma_i(\text{expt})/\sigma_i(\text{Born})$ is the empirical factor of correction,

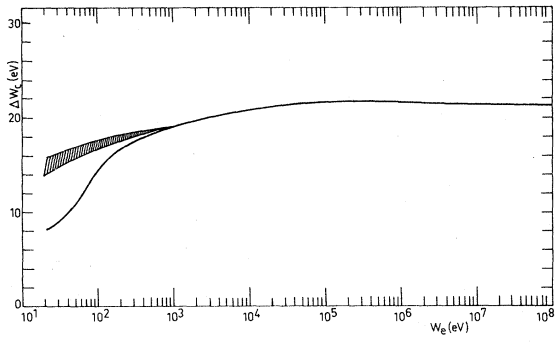

FIG. 2. Mean energy loss per collision ΔW_c of electrons in hydrogen. $\Delta W_c = (1/n\sigma_T)(dW_e/ds)$ is plotted versus the electron energy W_e. Full line curve is obtained by using theoretical cross sections (Ref. 10). By dashes are represented ΔW_c values obtained from experimental data on ionization cross sections of atomic hydrogen (Ref. 22).

$q = 1.60210\ 10^{-19}$ C is the electronic charge, $I_H = R\hbar = 13.5$ eV is the hydrogen ionization potential, R is the Rydberg frequency, Z is the atomic number, σ_i(expt) is the experimental ionization cross section, σ_i(Born) is the theoretical ionization cross section computed by the Born approximation, and $\epsilon_0 = 8.859\ 10^{-12}$ F m^{-1} is the vacuum permittivity. The empirical factor K_1 for H_2 takes a value between 0.5 and unity for the energy range from 50 to 100 eV. It is almost equal to unity for higher energies. For N_2 and CO_2, K_1 is taken equal to unity. For the atomic hydrogen, the electron energy loss per collision

$$\Delta W_e = \frac{1}{n\sigma_T}\,\frac{dW_e}{ds}$$

is plotted in Fig. 2 versus the electron energy W_e.[10]

B. Low Energy

The Born approximation fails at electron energies smaller than 80–50 eV. The electron energy-loss rate can be evaluated by summing all the possible energy-loss mechanisms of an electron interacting with an atom or a molecule:

$$\frac{dW_e}{ds} \simeq -n\sigma_T\left((V_i + W_{s0})\,\alpha_i + \sum_{m,n} V_{m,n}^{*}\,\alpha_{m,n} + 2\,\frac{m_e}{M}\,W_e\,\alpha_d\right)\ \text{eV m}^{-1}\ , \quad (3.2)$$

where σ_T is the total collision cross section. This method requires knowledge of the ionization cross section $\alpha_i\,\sigma_T$, the mean initial energy W_{s0} of the electron ejected in an ionizing collision, the excitation cross sections $\alpha_{m,n}\,\sigma_T$ (excluding ionization), and the momentum-transfer cross section $\alpha_d\,\sigma_T$. V_i and $V_{m,n}$ are, respectively, the ionization potential and the excitation energy from the mth to the nth level; m_e and M are, respectively, the mass of the electron and of the cluster molecules. The ionization cross sections for H_2, N_2, and CO_2 are given in the literature.[11] Only the terms corresponding to transitions from the ground level to the first few excited levels give significant contributions to the formula (3.2). The values of the cross sections we use are those assumed by Phelps and co-workers in their analysis of the experimental data on electron swarms in H_2, N_2, CO_2.[12–14] For each molecular species, these values are a coherent set of cross sections for the different electron-molecule interactions. Detailed discussion on the method of analysis employed in establishing these sets of cross sections is given in the original papers. The momentum-transfer term by elastic scattering is always negligible for W_e greater than a few electron volts. The dependence of dW_e/ds on the electron energy W_e is shown in Figs. 3–5, respectively, for H_2, N_2, CO_2 clusters. The values of dW_e/ds for N_2 and CO_2 from 30 to 80 eV are computed with poor accuracy (errors $\leq 50\%$) due to the lack of precise data. Nevertheless, the energy-loss rate in this region affects the cluster ionization cross sections only slightly for initial electron energy greater than 100 eV. Moreover, the secondary-electron mean energy is always less than 30 eV. Hence, this region is not important for the results of our calculations. The energy-loss rate of electrons can be approximated in this region by the formulas given in Table I.

C. Very Low Energy

Electrons whose energy is smaller than 5–10 eV lose their energy mainly by excitation of the vibrational and rotational levels of the molecules. The elastic momentum transfer is no longer negligible, and it becomes more and more important as the electron energy is decreasing. The en-

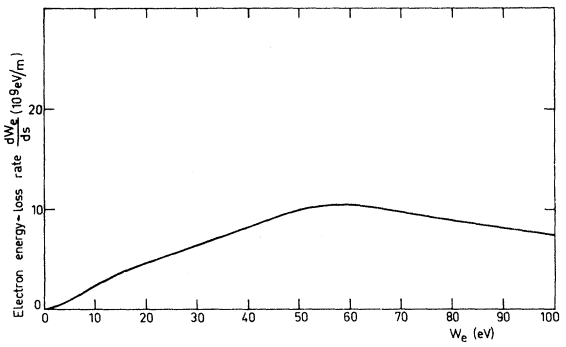

FIG. 3. Energy-loss rate dW_e/ds for low-energy electrons in H_2 versus the electron energy W_e (W_e in eV; dW_e/ds in eV m^{-1}).

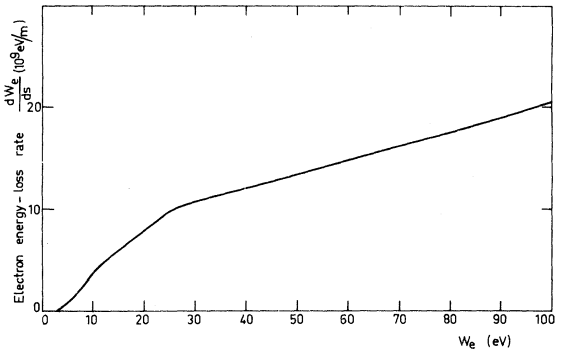

FIG. 4. Energy-loss rate dW_e/ds for low-energy electrons in N_2 versus the electron energy W_e (W_e in eV; dW_e/ds in eV m^{-1}).

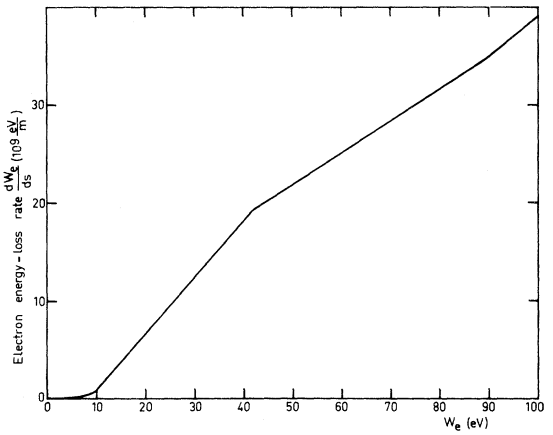

FIG. 5. Energy-loss rate dW_e/ds for low-energy electrons in CO_2 versus the electron energy W_e (W_e in eV; dW_e/ds in eV m^{-1}).

ergy-loss rate can be expressed in the following form:

$$\frac{dW_e}{ds} \simeq -\frac{W_e}{v_e}\left(\frac{\nu_u}{n_0}\right) n_0 \text{ eV m}^{-1} \ , \qquad (3.3)$$

where ν_u is the energy-exchange collision frequency, as defined and evaluated by Phelps and co-workers for electrons in several gases.[12,13,15] The energy-loss rate dW_e/ds vs W_e is shown in Figs. 6–8, respectively, for electrons in H_2, N_2, and CO_2. These values can be approximated by the formulas given in Table II.

IV. ELECTRON SCATTERING

A. High Energy

The differential cross sections fall off with increasing scattering angle more rapidly for inelastic than for elastic collisions. Therefore the standard deviation α of the resultant scattering angle after n collisions has been evaluated for elastic collisions only. By using William's approximate form for the elastic scattering differential cross section,[16] the value of α is found approximatively equal to $\theta_1 n^{1/2}$, where $\theta_1 = A_c/180 v_e$[16]; c and v_e are, respectively, the light and the electron velocity; and $A \simeq Z^{1/3}$. Accurate values of A for several atoms are given in Ref. 16. Below 100 eV, α/n is about 10°; however in a spherical cluster the effective length of the electron trajectories differs on the average from the mean unscattered path ($\simeq 0.62D$, where D is the cluster

TABLE I. Energy-loss rate for electrons of low energy (dW_e/ds in eV m^{-1}; W_e in eV).

Hydrogen clusters (H_2)
$\frac{dW_e}{ds} \simeq -(1+0.18W_e)\times 10^9 \quad 10 < W_e \leq 60$
Nitrogen clusters (N_2)
$\frac{dW_e}{ds} \simeq -(7+0.135W_e)\times 10^9 \quad 25 < W_e \leq 80$
$\frac{dW_e}{ds} \simeq -0.4\times 10^9 W_e \quad 10 < W_e \leq 25$
Carbon dioxide clusters (CO_2)
$\frac{dW_e}{ds} \simeq -(4.8+0.35 W_e)\times 10^9 \quad 40 < W_e \leq 90$
$\frac{dW_e}{ds} \simeq -(-3.72+0.53 W_e)\times 10^9 \quad 20 < W_e \leq 40$
$\frac{dW_e}{ds} \simeq -(-4.9+0.59 W_e)\times 10^9 \quad 10 < W_e \leq 20$

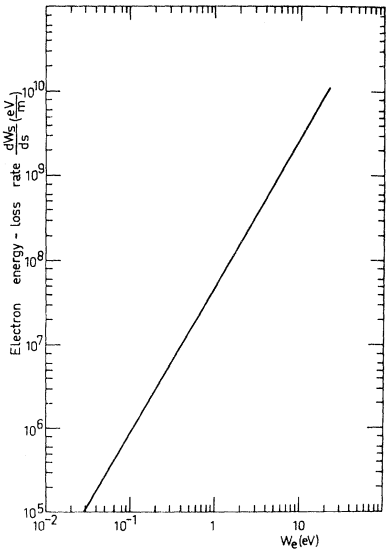

FIG. 6. Energy-loss rate dW_e/ds for electrons of very low energy in H_2 versus the electron energy W_e (Ref. 12) (W_e in eV; dW_e/ds in eV m^{-1}).

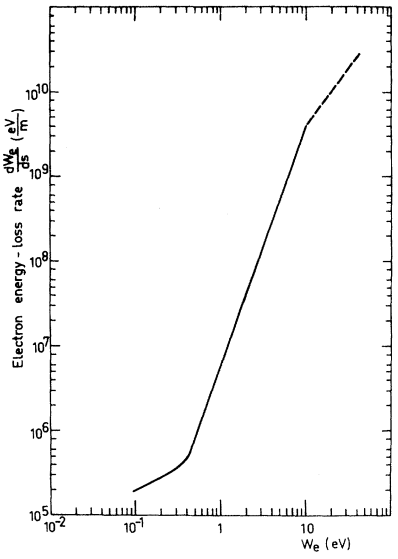

FIG. 7. Energy-loss rate dW_e/ds for electrons of very low energy in N_2 versus the electron energy W_e (Ref. 13) (W_e in eV; dW_e/ds in eV m^{-1}).

diameter) by less than 10%. So we assume in our calculations that the primary-electron trajectories are always linear down to about 50 eV.

B. Low Energy

The electron scattering for $W_e < 30$ eV has been evaluated taking into account the molecular structure of the cluster. In H_2, N_2, and CO_2 crystals, molecules are tied to each other by the van der Waals forces. The corresponding cohesive energies are about 10^{-2} to 10^{-1} eV per molecule. An electron passing through the solid lattice induces dipole moments in the surrounding molecules. One can define a minimum impact parameter b^* in the induced dipole field such that electrons with an impact parameter $b < b^*$ spend a very long time interacting with a molecule as they spiral around it until they are repelled by the molecular potential.[17] The value of b^* is as follows:

$$b^* \simeq 4.95\times10^{-3}\left(\frac{\epsilon_r - 1}{\epsilon_r}\,\frac{1}{n_0}\,\frac{1}{W_e}\right)^{1/4} \text{m}$$

(W_e in eV) ,

where ϵ_r is the relative cluster dielectric constant. The dependence of b^* on W_e, computed on a line joining two molecules, is shown in Fig. 9. Electrons with $b < b^*$ are scattered through an angle θ, expressed in the c.m. system by

$$\theta = \pi - 2\int_0^{\rho_0} \frac{d\rho}{[1-\rho^2+\frac{1}{4}\rho^4(b^*/b)^4]^{1/2}} , \qquad (4.1)$$

with $\rho = b/r$. r is the distance from the electron to the molecule. For energies smaller than 30 eV, which include always secondary electrons, the scattering angles fall between 30° and 180° for $b^* < b < \frac{1}{2}d_0$. Since b^* is about $\frac{1}{2}d_0$, where d_0 is the intermolecular distance, scattering angles are, in general, very large. In fact, if an electron has an impact parameter greater than b^* with respect to the nearest molecule, the probability of passing at a distance $\gg b^*$ from the next center of scattering is very low. The probability that an electron can escape from the cluster without passing closer than b to one molecule is roughly

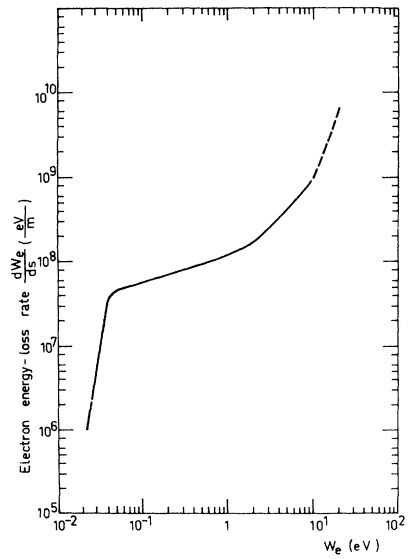

FIG. 8. Energy-loss rate dW_e/ds for electrons of very low energy in CO_2 versus the electron energy W_e (Ref. 15) (W_e in eV; dW_e/ds in eV m^{-1}).

TABLE II. Energy-loss rate for electrons of very low energy (dW_e/ds in eV m^{-1}; W_e in eV).

Hydrogen clusters (H_2)

$$\frac{dW_e}{ds} \simeq -4.9\times10^{7}\, W_e^{1.75} \quad 10^{-2} \le W_e \le 10$$

Nitrogen clusters (N_2)

$$\frac{dW_e}{ds} \simeq -4\times10^{5}(2.5W_e)^{2.9} \quad 0.4 < W_e \le 10$$

$$\frac{dW_e}{ds} \simeq -2\times10^{5}(10W_e)^{0.5} \quad 0.1 < W_e \le 0.4$$

Carbon dioxide clusters (CO_2)

$$\frac{dW_e}{ds} \simeq -3.2\times10^{8}(0.25W_e)^{1.24} \quad 4 < W_e \le 10$$

$$\frac{dW_e}{ds} \simeq -1.2\times10^{8}W_e^{0.7} \quad 1 < W_e \le 4$$

$$\frac{dW_e}{ds} \simeq -4.3\times10^{7}(25W_e)^{0.32} \quad 0.04 < W_e \le 1$$

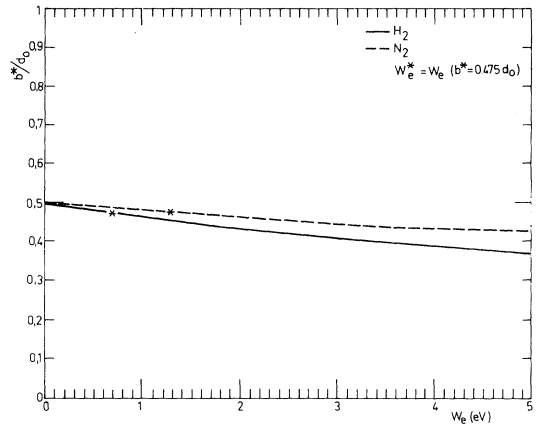

FIG. 9. Minimum impact parameter b^* in electron-molecule interaction versus the electron energy W_e, for H_2 and N_2. b^* is computed in the dipolar potential induced by an electron on a line joining two molecules a distance d_0 from each other. At $\frac{1}{2}d_0$ the electron does not interact with the two molecules because the two induced potentials cancel mutually (W_e in eV; b^* in units of d_0, the intermolecular distance).

$$P_u \simeq \frac{1-(2b/d_0)^2}{2g^2}\,, \qquad (4.2)$$

where g is the distance (normalized to d_0) from the electron to the cluster surface. In the range of energy of the ejected electron $P_u \leq 5\times10^{-2}$ if $g \geq 2$. Therefore the electrons of less than 30 eV experience large-angle scattering each time they collide with a molecule of the crystal lattice. As the total collision cross-section magnitude is about the mesh area of the crystal lattice, the mean free path for a scattering collision is the intermolecular distance d_0. We have thereafter assumed that the motion of the low-energy electrons inside the cluster looks like a three-dimensional random walk, with a mean free path equal to d_0.

V. SECONDARY-ELECTRON ENERGY

In order to calculate the cluster ionization cross section, it is necessary to evaluate the range of the secondary electrons. To do this, the initial energy W_{s0} of the secondary electrons must be known to compute dW_e/ds from formula (3.2). For hydrogen, in the range 50–10^4 eV, dW_e/ds is given by Bethe's formula [Eq. (3.1)], and the dependence of the ionization and excitation cross sections on the electron energy is known theoretically. It is then possible to compute the relation between W_{s0} and W_e from formula (3.2). This is not possible for energies lower than 50 eV because Bethe's formula is no longer valid. Between the ionization potential V_i, for which $W_{s0} = 0$, and $W_e = 50$ eV, we arbitrarly use an interpolation. The ejected-electron mean initial energy W_{s0} versus W_e is shown in Fig. 10. The curves show good agreement with those deduced from the velocity distributions calculated for electrons ejected in ionizing collisions with hydrogen atoms.[19] The values of W_{s0}, calculated at a given W_e in the region 50–200 eV, are spread between 12 and 20 eV, depending mainly on the chosen value of the ionization cross section (theoretical or experimental). Though precise experimental informations on the energy spectrum of the ejected electrons is lacking, the trend found for W_{s0} vs W_e agrees with the available experimental data.[20]

The energy spectrum of the secondary electrons measured in several gas targets does not seem to show any significant dependence on the nature of the gas. In formula (3.2) the weight of the ejected-electron term never exceeds 35–40% of the total loss, hence the accuracy in W_{s0} which is always better than 30% affects, only slightly, the estimation of dW_e/ds in the low-energy region. In addition, we shall show that the range of the secondary electron in the cluster depends rather more on the rate of energy loss than on the initial mean kinetic energy W_{s0} of the ejected electron. Hence we assume the calculated relationship between W_s and W_e is adequate for our use and holds approximatively for N_2 and CO_2 also. We can write $W_{s0} = f_1(W_e)$ as follows:

$$W_{s0} \simeq 10 + 3.33\ln(0.032W_e)\ \text{eV}, \qquad 50\ \text{eV} < W_e \leq 10^4\ \text{eV} \qquad (5.1)$$

$$W_{s0} \simeq 8.8\ln(0.074W_e)\ \text{eV}, \quad V_i < W_e \leq 50\ \text{eV}.$$

VI. RANGE OF ELECTRONS

An electron, losing energy by collisions with the crystal lattice, is stopped before reaching the cluster surface when its energy becomes smaller than some critical value W^*, which is the largest

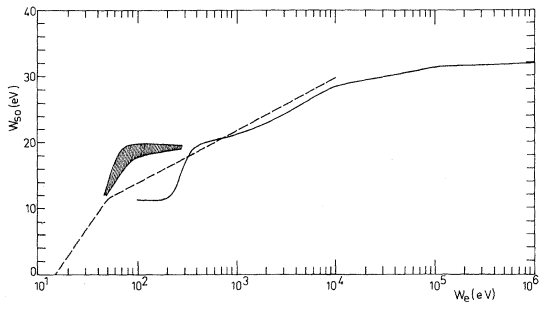

FIG. 10. Mean kinetic energy of the ejected electron W_{s0} versus the energy of the primary electron W_e. Solid line curve is obtained by using theoretical cross sections (Ref. 10). W_{s0} evaluated by using experimental data on atomic hydrogen ionization cross section (Ref. 18) is plotted by dashes. Dotted line represents the averaged values of W_{s0} used in computations.

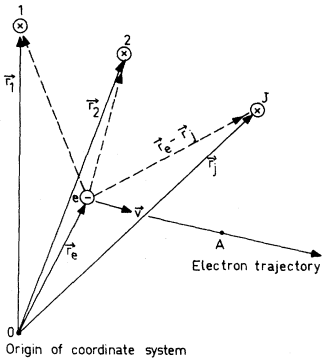

FIG. 11. Coordinate system for an electron interacting with several electric charges.

value determined by the following conditions:

(a) The electron becomes trapped in the Coulomb potential of one or several ions, which can be the cluster electrical charges or the ion resulting from the considered ionizing collision. In this case W^* depends on the electron position.

(b) For low electron energy ($\simeq 1$ eV) the minimum impact parameter b^* is very close to $\frac{1}{2}d_0$ so that an electron spends a long time in spiral orbits around molecules. As vibrational and rotational levels of the molecule can still be excited, we suppose that the electron keeps on in losing energy along its trajectory. As the minimum impact parameter b^* increases with decreasing energy, the probability for the electron to collide with an impact parameter $b^* < b < \frac{1}{2}d_0$ becomes rapidly negligible. Therefore, the electron can be considered trapped in the dipole potential of one of the surrounding molecules, as soon as its energy is so low that b^* becomes close to $\frac{1}{2}d_0$. Values of $2b^*/d_0$, for which the electron trapping in the induced dipole potential is effective, are given later.

A. Trapping in Coulomb Field

The energy equation of an electron in a Coulomb field of n fixed positive charge would be, in the absence of energy losses,

$$W_{e\infty} = W_e - \frac{q_e}{4\pi\epsilon}\sum_1^n{}_j \frac{q_j}{|\vec{r}_e - \vec{r}_j|}, \qquad (6.1)$$

where $\vec{r}_j$ are the vectors defining the position of the fixed charges and $\vec{r}_e$ is the vector defining the position of the electron (Fig. 11). W_e is the local kinetic energy of the electron; $W_{e\infty}$ is the electron kinetic energy at the infinity.

Inside the cluster, electrons lose their kinetic energy at a rate dW_e/ds at the same time that they change their potential energy in the Coulomb field. If A is the starting point of the electron path inside the cluster and W_{eA} is the electron kinetic energy at A, Eq. (6.1) must be modified as follows:

$$W_e = W_{eA} - \frac{q_e}{4\pi\epsilon}\left(\sum_1^n{}_j \frac{q_j}{|\vec{r}_e - \vec{r}_j|} - \sum_1^n{}_j \frac{q_j}{|\vec{r}_{eA} - \vec{r}_j|}\right) - \int_{W_{eA}}^{W_e} \frac{dW_e}{ds}\, ds, \qquad (6.2)$$

where

$$W_{eA} - \sum_1^n{}_j \frac{qq_e}{4\pi\epsilon}\frac{1}{|\vec{r}_{eA} - \vec{r}_j|} = W_\infty .$$

The electron is trapped when

$$W_e \leq \frac{|q_e|}{4\pi\epsilon}\sum_1^n{}_j \frac{q_j}{|\vec{r}_e - \vec{r}_i|} = W^*, \qquad (6.3)$$

that is, when its kinetic energy is lower than the depth of the Coulomb potential at the point $\vec{r}_e$.

The following system must be solved to know the electron kinetic energy along its trajectory:

$$W_e = W_{eA} - \frac{q_e}{4\pi\epsilon}\left(\sum_1^n{}_j \frac{q_j}{|\vec{r}_e - \vec{r}_j|} - \sum_1^n{}_j \frac{q_j}{|\vec{r}_{eA} - \vec{r}_j|}\right) - \int_{W_{eA}}^{W_e} \frac{dW_e}{ds}\, ds , \qquad (6.4)$$

$$\frac{dW_e}{ds} = f_1(W_e), \quad s = f_2(\vec{r}_e) ,$$

with the boundary conditions

$$\vec{r}_e = \vec{r}_{eA} , \quad \vec{s} = 0 , \quad W_e = W_{eA} .$$

[The last condition is already included in (6.2).] The trapping condition (6.3) determines a function

$$\vec{r}_{ef} = f_3(|\vec{r}_{eA} - \vec{r}_j|, W_{eA}, \epsilon, d_0),$$

and the range is then

$$\mathcal{R} = |\vec{r}_{ef} - \vec{r}_{eA}| . \qquad (6.5)$$

The system (6.4) is very difficult to solve in all but a few simple cases. However the actual situations in a cluster are simple. In fact small clusters can carry, without breaking up, only one positive electrical charge[4] while large ones can only carry a few charges ($N \geq 10^3$ molecules).[8,9]

The range $\mathcal{R}$ defined in (6.5) depends on the position of the positive charge with respect to the electron trajectory. Therefore $\mathcal{R}$ must be averaged over all possible electron trajectories and all possible charge configurations. The dependence of $\mathcal{R}$ on the physical properties of the cluster is included in the dielectric constant ϵ, the intermolecular distance d_0, and W_{eA}, which, in the case of a secondary electron, includes the ionization potential of the cluster molecule [see Eq. (6.7)].

In this work we have solved the system (6.4) for a cluster with one positive charge and the secondary electron resulting from the formation of this

positive charge. For the case of a secondary electron resulting from the ionization of the mth molecule equation, (6.2) becomes

$$W_s = W_{sm} + \frac{a_e}{4\pi\epsilon}\left(\sum_1^n{}_j \frac{q_j}{|\vec{r}_e - \vec{r}_j|} - \sum_{1\ j\neq m}^{n} \frac{q_j}{|\vec{r}_m - \vec{r}_j|}\right) - V_{im} - \int_{W_{sm}}^{W_s} \frac{dW_s}{ds}\, ds \qquad (6.6)$$

because

$$\frac{1}{4\pi\epsilon_0}\ \frac{q^2}{|\vec{r}_{eA} - \vec{r}_m|} = V_{im},$$

the ionization potential of the m molecule, and

$$r_{eA} \simeq r_m\ , \qquad W_{sm} \simeq V_{im} + W_{s0}\ , \qquad (6.7)$$

where W_{s0}, the secondary-electron energy, is determined by formulas (5.1).

If $n = 1$ we have

$$W_s = (V_1 + W_{s0}) - \frac{a^2}{4\pi\epsilon|\vec{r}_e - \vec{r}_i|} - V_i - \int_{V_i + W_{s0}}^{W_s} \left(\frac{dW_e}{ds}\right) ds\ , \qquad (6.8)$$

$$\frac{dW_s}{ds} = f_1(W_s)$$

(the equation is given in Table I or II depending on the values of W_e and on the nature of the cluster),

$$s = f_2(\vec{r}_2)\ .$$

As shown in Sec. IV, the path of the secondary electrons inside the cluster can be considered as a random walk in three dimensions with $\lambda \simeq d_0$. Therefore

$$s \simeq n d_0\ ,$$

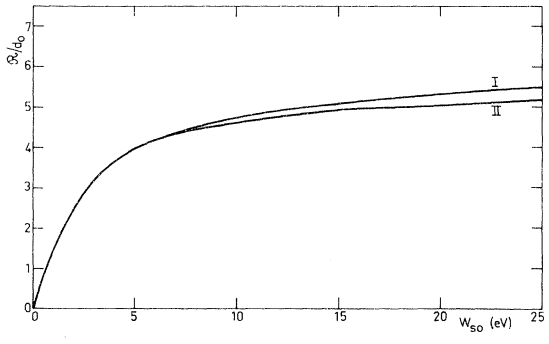

FIG. 12. Range $\mathfrak{R}$ of secondary electrons in H_2 clusters versus electron energy W_{s0}. W_{s0} is the kinetic energy (at infinity) of the electron at its ejection from the molecule. (W_{s0} in eV; $\mathfrak{R}$ in units of d_0, the intermolecular mean distance.) Curve I: Coulomb trapping; curve II: dipole field trapping ($b^* = 0.475 d_0$).

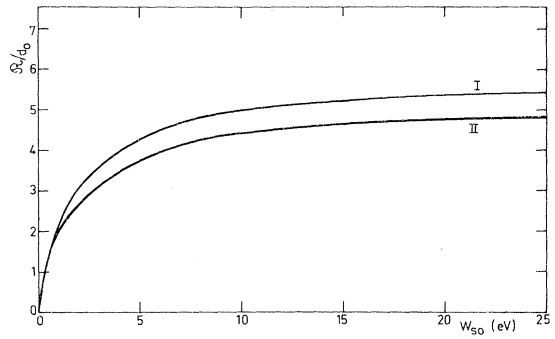

FIG. 13. Range $\mathfrak{R}$ of secondary electrons in CO_2 clusters versus electron energy W_{s0}. W_{s0} is the kinetic energy (at infinity) of the electron at its ejection from the molecule. (W_{s0} in eV; $\mathfrak{R}$ in units of d_0, the intermolecular mean distance.) Curve I: Coulomb trapping; curve II: dipole field trapping ($b^* = 0.475 d_0$).

$$|\vec{r}_e - \vec{r}_i| \simeq (\tfrac{1}{3}n)^{1/2} d_0\ ,$$

where n is the number of collisions and $s = f_2(\vec{r}_e)$ becomes

$$s = (3/d_0)|\vec{r}_e - \vec{r}_i|^2\ .$$

Figures 12 and 13 show, respectively, the values of $\mathfrak{R}/d_0$ for clusters of H_2 and CO_2 (curve I) versus the secondary-electron energy W_{s0}; beyond this distance the secondary electron has lost enough kinetic energy to be recaptured in the Coulomb field of the ion produced by ionization. As the electron starts from the ion position, we have only one possible relation between the electron trajectory and the ion position.

Tay *et al.*[7] and Falter *et al.*[8] point out that experimental cross sections for H_2 and CO_2 clusters have values such that one can consider the cluster ionization to be effective only in an outer shell of thickness three or four times d_0. It is noteworthy that this qualitative picture agrees with the electron range computed by our model, which takes into account the microscopic behavior of electrons inside the cluster.

B. Trapping in Dipole Field

Electrons can be trapped not only in the Coulomb potential of an ion but in the dipole potential (induced by the electron itself) of a molecule. When the electron energy becomes so low that the corresponding minimum impact parameter $b^*(W_e)$ is close to $\frac{1}{2}d_0$ the electrons can be considered as trapped. The trapping probability evaluated for H_2 and CO_2 from the Coulomb potential agrees very well with the experimental data.

The trapping in the Coulomb field is effective when the secondary-electron energy becomes on the average smaller than $W^* \simeq 0.7$ eV for H_2 and $W^* \simeq 1.2$ eV for CO_2. The minimum impact pa-

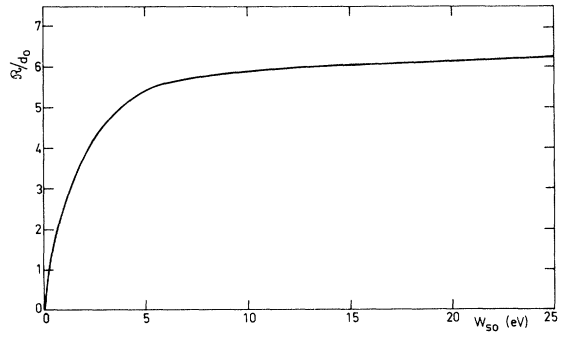

FIG. 14. Range $\mathcal{R}$ of secondary electrons in N_2 clusters versus the electron energy W_{s0} (dipolar potential trapping). Electron is captured when $b^* = 0.475 d_0$, that is, when $W_s \simeq 1.3$ eV. W_{s0} is the kinetic energy (at infinity) of the electron at its ejection from the molecule. (W_{s0} in eV; $\mathcal{R}$ in units of d_0, the intermolecular mean distance.)

rameters corresponding to these energies are almost the same for H_2 and CO_2 and equal to $b^* \simeq 0.475 d_0$. Because of the very rapid variation of W_e vs b^* near $b^* \simeq \frac{1}{2} d_0$ these data are not very accurate. Figures 12 and 13 (curves II) show the range $\mathcal{R}/d_0$ vs W_{s0} obtained by taking exactly $W^* = 0.7$ eV for H_2 and $W^* = 1.2$ eV for CO_2, that is, by choosing as the electron-energy limit the one corresponding to a minimum impact parameter $b^* \simeq 0.475 d_0$. The difference between curves I and II is not significant, and it is due to our approximations used for choosing b^*.

For N_2 the trapping probability calculated in the Coulomb potential or in the dipole potential with $b^* \geq 0.475 d_0$ ($W^* \leq 1.3$ eV, see Fig. 9) are very different. Figure 14 shows R/d_0 vs W_{s0} calculated for nitrogen by the dipole potential trapping. $\mathcal{R}/d_0$ is of the same order of magnitude for the results in H_2 and N_2 obtained by the Coulomb potential trapping. Values of $\mathcal{R}/d_0$ calculated for several limiting energies W^* are given in Fig. 15. The limiting energy in the Coulomb potential is $W^* \simeq 0.1$ eV and the corresponding $\mathcal{R}/d_0$ is 35, that is about seven times greater than for H_2 and CO_2 at the same electron initial energy $W_{s0} = 10$ eV. The lack of experimental results for N_2 clusters does not allow us to choose at present between the two methods of determining the range of the low-energy electrons.

The trapping of electrons in N_2 seems likely to occur owing to the dipole potential since it acts before the Coulomb trapping, whereas in H_2 and CO_2 the trapping seems to be due to the Coulomb potential.

To compute the range for a secondary electron in the dipole field one must solve the system (6.4) coupled to the trapping condition

$$W_s < W^* \quad (b^* = 0.475\, d_0) \tag{6.9}$$

instead of condition (6.3).

C. Range of Primary Electrons

The range of primary electrons of energy higher than about 80–100 eV is very large because the path of the scattered electrons is not a random walk. The trapping conditions give values of $\mathcal{R} \geq (200\text{–}300) d_0$. Primary electrons could then be captured only in clusters for which the mass number is $N \geq 10^8$ molecules. These clusters are at least of three orders of magnitude greater in size than the clusters produced in present systems.

VII. RESULTS OF NUMERICAL COMPUTATIONS

Computations of the cluster ionization cross section under electronic impact has been performed on a IBM 360-91 computer for H_2, N_2, and CO_2. The double integration of (2.11) is performed by the trapezium method. At each j step over x, the electron energy W_{ej} is obtained by integrating the differential equation $dW_e/dx = f(W_e)$, where $f(W_e)$ is one of the equations of Tables I and II. This integration is performed by the Runge–Kutta method with four orders of approximation. At each j step over x, W_{ej}, $F(W_{ej}, x_j)$, and $\sigma(1, W_{ej})$ are calculated.

The computed values of $\sigma(N, W_{e0})/\sigma(N, W_{eM})$ versus the initial electron energy W_{e0} for several molecular number of mass N are plotted in Figs. 16–18, respectively, for H_2, CO_2, and N_2 clusters. The values $\sigma(1, W_{e0})/\sigma(1, W_{eM})$ for the corresponding molecules are shown on the same figures as well as the experimental results available for

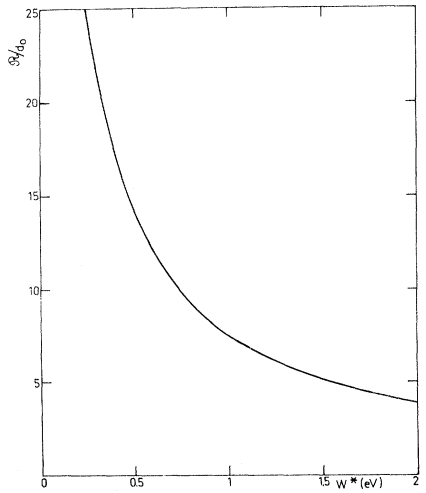

FIG. 15. Range $\mathcal{R}$ of secondary electrons in N_2 clusters versus arbitrary limit energies W^*. $W_{s0} = 10$ eV. (W^* in eV; $\mathcal{R}$ in units of d_0, the intermolecular mean distance.)

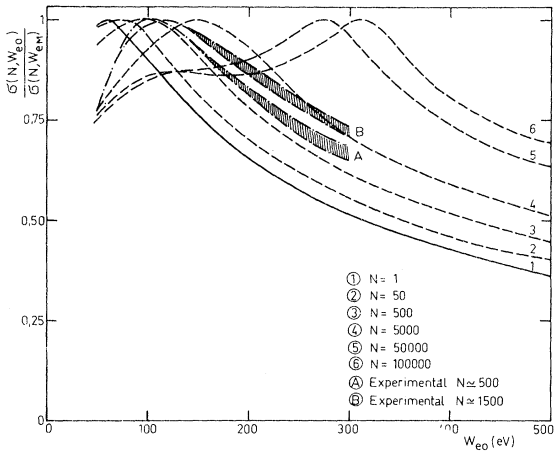

FIG. 16. Computed ionization cross section $\sigma(N, W_{e0})$ of H_2 cluster by electron impact versus the initial electron energy W_{e0}. $\sigma(N, W_{e0})$ is normalized to the maximum cross section $\sigma_{max} = \sigma(N, W_{eM})$. On this figure are drawn $\sigma(1, W_{e0})$, the molecular ionization cross section by electron impact, normalized to its maximum $\sigma(1, W_{eM})$, and the experimental data of Tay *et al.* (Ref. 7) for H_2 clusters (W_{e0} in eV).

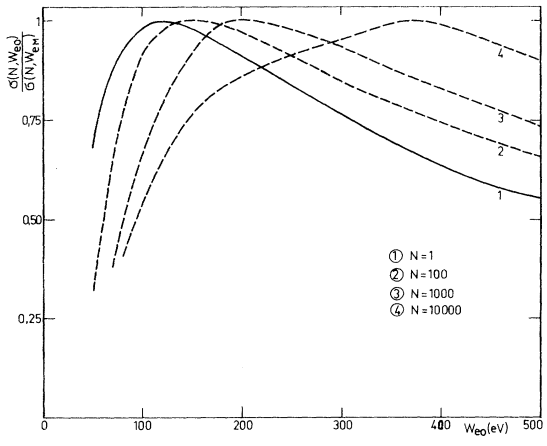

FIG. 18. Computed ionization cross section $\sigma(N, W_{e0})$ of N_2 clusters by electron impact versus the initial electron energy W_{e0}. $\sigma(N, W_{e0})$ is normalized to the maximum cross section $\sigma_{max} = \sigma(N, W_{eM})$. $\sigma(N, W_{e0})$ is computed by taking into account the values of $\mathcal{R}$ of Fig. 13 (electron trapping in the dipole field). On this figure is drawn the molecular cross section $\sigma(1, W_{e0})$ normalized to its maximum $\sigma(1, W_{eM})$ (W_{e0} in eV).

H_2[7] and CO_2[8] clusters: The agreement between the computed and the experimental data is fairly good, especially for W_e greater than W_{eM}, the energy corresponding to the maximum of the cluster cross sections.

The dependence of W_{eM} on the cluster mass number, shown on Figs. 19–21, is in agreement with the available experimental data.

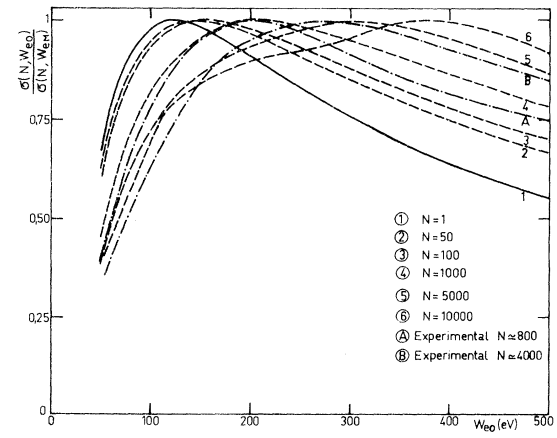

FIG. 17. Computed ionization cross section $\sigma(N, W_{e0})$ of CO_2 clusters by electron impact versus the initial electron energy W_{e0}. $\sigma(N, W_{e0})$ is normalized to the maximum cross section $\sigma_{max} = \sigma(N, W_{eM})$. On this figure are drawn $\sigma(1, W_{e0})$, the molecular ionization cross section normalized to its maximum $\sigma(1, W_{eM})$, and the experimental data of Falters *et al.* (Ref. 8) for CO_2 clusters (W_{e0} in eV).

The ratios of cluster ionization cross sections over the corresponding molecular ionization cross section $\sigma(N, W_{e0})/\sigma(1, W_{e0})$ are plotted versus N in Figs. 22–24 for several initial energies W_{e0} of the primary electrons. For very small clusters $\sigma(N, W_{e0})/\sigma(1, W_{e0})$ is proportional to N, whereas for larger clusters it increases more slowly than N. In the range $10^2 < N < 10^4$ the slope of $\sigma(N, W_{e0})/\sigma(1, W_{e0})$ is roughly proportional to $N^{2/3}$.

The experimental data available for H_2 clusters[7] agree fairly well with the calculated ones. For CO_2 the experimental values have been plotted in Fig. 23 by assuming the cluster to be multicharged. The measured decrease of N/Z when W_{e0} grows has been interpreted as due to an in-

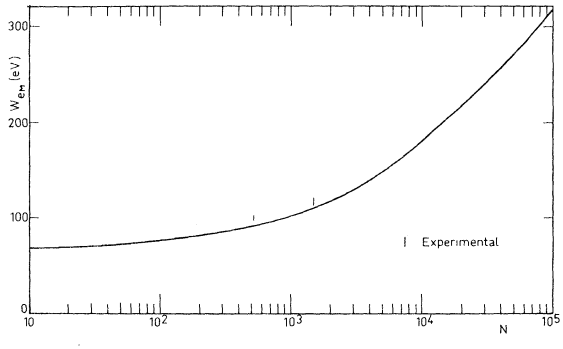

FIG. 19. Computed energy W_{eM} corresponding to the maximum ionization cross section of H_2 clusters by electron impact versus the cluster molecular mass number N (W_{eM} in eV).

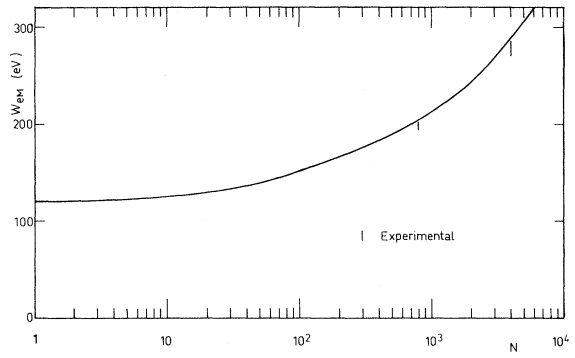

FIG. 20. Computed energy W_{eM} corresponding to the maximum ionization cross section of CO_2 clusters by electron impact versus the cluster molecular mass number N (W_{eM} in eV).

crease of Z, rather than to a reduction of the cluster number of mass.[8] The experimental curve on Fig. 23 for $W_e = 100$ eV has been inferred from the data given in papers.[21]

The discrepancies between the experimental and calculated values are due likely to experimental errors, mainly in estimating the cluster mass number, as well as to the approximations of the present model. We recall that the ionization cross sections are computed for a fixed cluster mass or for a Poisson distribution of the masses, whereas experiments deal with the mean value of the actual distribution function. This latter has not been directly measured; only its possible shape has been inferred by difficult elaborations of the crude experimental data.[7,8,21]

It is possible to make the computed values fit the experimental ones by adjusting empirically the energy-loss rates and the electron scattering; nevertheless we believe these numerical corrections are at present meaningless because more experimental data are necessary, in particular, those concerning cluster beams of well-defined mass.

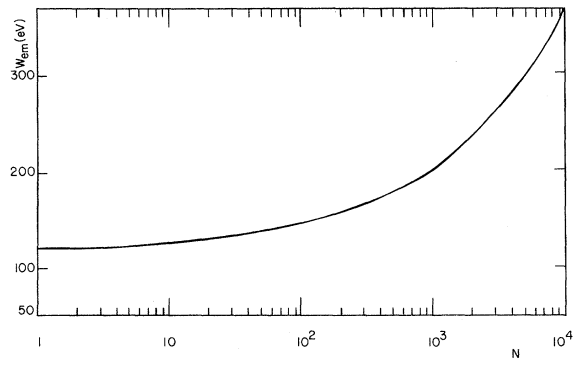

FIG. 21. Computed energy W_{eM} corresponding to the maximum ionization cross section of N_2 clusters by electron impact versus the cluster molecular mass number N (W_{eM} in eV).

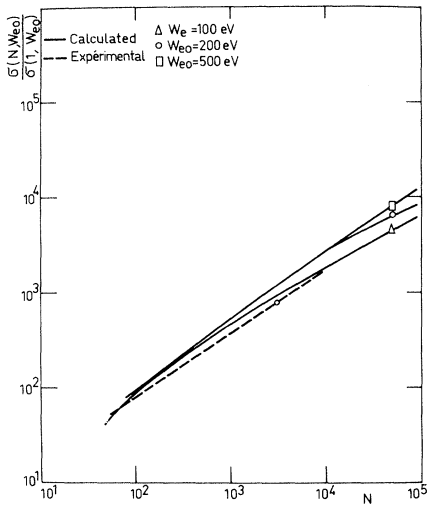

FIG. 22. Computed ionization cross section of H_2 clusters by electron impact $\sigma(N, W_{e0})$ versus the clusters molecular mass number N, for electron initial energy $W_{e0} = 100$, 200, 500 eV. $\sigma(N, W_{e0})$ is normalized to the value of the corresponding molecular ionization cross section at the same electron energy W_{e0}. In this figure are drawn the experimental data of Tay *et al.* (Ref. 7) at $W_{e0} = 200$ eV.

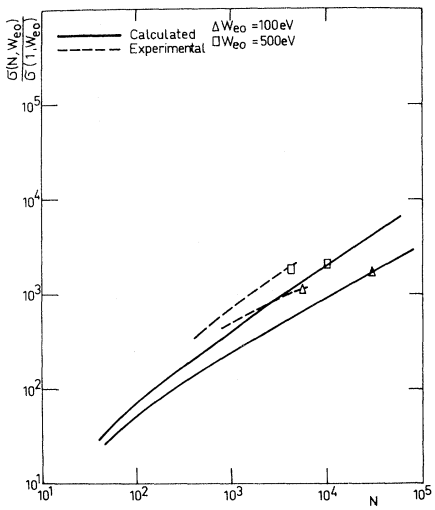

FIG. 23. CO_2 cluster ionization cross section $\sigma(N, W_{e0})$, computed for electron impact, versus the cluster molecular mass number N, for electron initial energies $W_{e0} = 100$ and 500 eV. $\sigma(N, W_{e0})$ is normalized to the value of the corresponding molecular ionization cross section at the same electron energy W_{e0}. In this figure are drawn the experimental data of Falter *et al.* (Ref. 8) at $W_{e0} = 500$ eV and Hagena (Ref. 21) at $W_{e0} = 100$ eV.

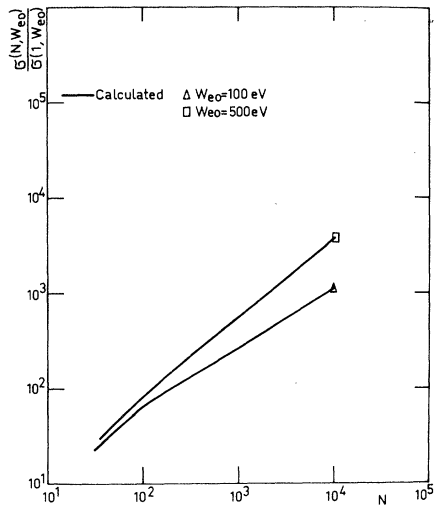

FIG. 24. N_2 cluster ionization cross section $\sigma(N, W_{e0})$, computed for electron impact, versus the cluster molecular mass number N, for electron initial energies W_{e0}: 100 and 500 eV. $\sigma(N, W_{e0})$ is normalized to the value of the corresponding molecular ionization cross section at the same electron energy W_{e0}.

VIII. CONCLUSIONS

The present model takes into account three simple phenomena: the energy loss of the electrons inside the cluster; the trapping of the secondary electrons, ejected in an ionizing collision, by the Coulomb field of the ion or by the induced dipole field of a cluster molecule; the random walk of the secondary electrons due to their large scattering. By evaluating numerically these three effects and by connecting them to each other, the present model allows one to estimate the probability for an electron, in particular a secondary electron, to escape from the cluster. It is then possible to evaluate the effective cluster ionization cross section defined in (1.2).

At the present state of experimental investigations of clusters under electron bombardment, we consider the agreement between the experimental and the computed values is fairly satisfactory.

A serious uncertainty in this model concerns the two kinds of electron trapping we suggest. For N_2 clusters, the ionization cross section should be very different depending on whether the Coulomb or dipole field traps electrons inside the cluster. This uncertainty can be removed only by experimental measurements. The cross section defined in Eq. (1.1) can be used to compute attenuation by ionization of a cluster beam, with mass number N or $\bar{N}$, whatever the cluster vaporization or splitting by multiple ionization may be. On the other hand this cross section may be used to compute the current of clusters, charged by ionization, only if cluster splitting by multiple ionization[6,9] and vaporization are negligible with respect to simple ionization. Indeed multiple ionization increases the current of charged particles and reduces their mass owing to splitting of the multicharged cluster, and vaporization lowers the cluster mass. We shall make some brief remarks on this latter problem.

Depending on their energy, the electrons excite mainly the electronic, vibrational, and rotational levels of the cluster molecules. The energy elastically transferred is not sufficient on an average to break the van der Waals forces binding the cluster molecules to one another. The electronic excitation energy probably does not increase the cluster internal energy because most of the molecular crystals are transparent.[22] Vibrational and rotational motions affect only slightly the position of the molecule mass centers inside the crystal lattice, therefore the crystal cohesive forces are not much perturbed. However, as these weak perturbations sum up at each electron-cluster collision it can be roughly estimated that a cluster evaporates or breaks up when the $n_e l$ value of the electron target is greater than about $10^{18} - 10^{19}\ m^{-2}$. However this is not the case of the experiments previously mentioned.[5,7-9,21]

The approximate dependence of the ionization cross section on $N^{2/3}$ for $N > 10^2$[7,8] is mainly due to the secondary-electron trapping. If the electron energy could be completely transferred to molecular kinetic energy, the clusters of $N < 10^3$ should vaporize at the first ionizing collision, contrary to the experimental evidence. Therefore it seems experimentally proved that the electron energy is dissipated essentially by mechanisms which do not affect strongly the cohesive forces of the crystal lattice.

[1]E. W. Becker, K. Bier, and W. Henkes, Z. Physik 146, 333 (1956).
[2]B. Raoult, J. Farges, and M. Rouault, Compt. Rend. 267B, 942 (1968).
[3]P. Audit, J. Phys. 30, 192 (1969).
[4]W. Henkes, Z. Naturforsch. 17a, 786 (1962).
[5]F. Bottiglioni, J. Coutant, M. Fois, and F. Prevot, in *Proceedings of the Fourth Conference on Plasma Physics and Controlled Nuclear Fusion Research, Madison, Wisconsin* (IAEA., Vienna, 1971), Vol. 2, p. 585.
[6]F. Bottiglioni, J. Coutant, and M. Fois, Proceedings of the Fourth Europeon Conference on Controlled Fusion and Plasma Physics, Rome, 1970, p. 96 (unpublished).
[7]E. S. Tay, P. G. Dawson, and G. A. G. Mosson, Proceedings of the Sixth European Symposium on Fusion Technology, Aachen, 1970 (unpublished).
[8]H. Falter, O. F. Hagena, W. Henkes, and H. V.

Wedel, Intern. J. Mass Spectry. Ion Phys. 4, 145 (1970).

[9]W. Henkes and G. Isenberg, Intern. J. Mass Spectry. Ion Phys. 5, 249 (1970).

[10]N. E. Mott and H. S. W. Massey, *The Theory of Atomic Collisions* (Clarendon, Oxford, 1952), pp. 248, 252, and 367.

[11]H. S. W. Massey, E. H. S. Burhop, and H. B. Gilbody, *Electronic and Ionic Impact Phenomena* (Clarendon, Oxford, 1969), Vol. II, Chap. 13, p. 910 for H_2, p. 972 for N_2, p. 1046 for CO_2.

[12]A. G. Engelhard and A. V. Phelps, Phys. Rev. 131, 2115 (1963).

[13]A. G. Engelhard, A. V. Phelps, and C. G. Risk, Phys. Rev. 135, A1566 (1964); see also Ref. 11, pp. 779, 984.

[14]R. D. Hake and A. V. Phelps, Westinghouse Research Report No. 66-1E2-P1, 1966 (unpublished); see also Ref. 11, pp. 1048, 792.

[15]R. D. Hake and A. V. Phelps, Phys. Rev. 158, 70 (1967).

[16]H. S. W. Massey and E. H. S. Burhop, *Electronic and Ionic Impact Phenomena* (Clarendon, Oxford, 1956), pp. 129 and 130.

[17]Earl W. McDaniel, *Collision Phenomena in Ionized Gases* (Wiley, New York, 1963), p. 72.

[18]W. L. Fite and R. T. Brackmann, Phys. Rev. 112, 1141 (1958); E. W. Rothe *et al.*, *ibid.* 125, 582 (1962).

[19]See Ref. 10, p. 236.

[20]D. R. Bates and G. W. Griffing, Proc. Phys. Soc. (London) A66, 961 (1953); A68, 90 (1955); D. R. Bates, M. R. C. McDowell, and A. Ornholt, J. Atm. Terrestr. Phys. 10, 51 (1957); M. R. C. McDowell and G. Peach, Phys. Rev. 121, 1383 (1961); see also Ref. 17, pp. 211 and 288.

[21]O. F. Hagena and W. Henkes, Z. Naturforsch. 20a, 1344 (1965); O. F. Hagena, Z. Angew. Phys. 16, 183 (1963).

[22]F. Seitz, *The Modern Theory of Solids* (McGraw-Hill, New York, 1940), pp. 72 and 635.

PHYSICAL REVIEW A VOLUME 6, NUMBER 5 NOVEMBER 1972

Exact and Semiempirical Analysis of the Generalized-Random-Phase-Approximation Optical Potential

György Csanak* and Howard S. Taylor*
Department of Chemistry, University of Southern California, Los Angeles, California 90007
(Received 20 March 1972)

A many-body optical potential Σ which has been demonstrated to give excellent electron-helium elastic scattering cross sections is analyzed. It is shown to encompass, yet be more general than, almost all previous model potentials used in electron scattering and Rydberg-state calculations. A partial semiempirical form of this potential is achieved. It is shown how Σ can be computed by methods of variation-perturbation theory.

I. INTRODUCTION

The recent numerical results for the properties of the helium system by Yarlagadda *et al.*[1] show the high physical quality of the optical potential Σ, the response R, and the Martin-Schwinger one-particle Green's function G, which were computed self-consistently in the generalized-random-phase-approximation (GRPA) method postulated by Schneider *et al.*[2] (This paper will be referred to later in the text as STY.) These quantities immediately yielded, in *simple* calculations, highly accurate elastic scattering cross sections, ionization energies, generalized oscillator strengths (hence Born inelastic scattering cross sections), ground-state energies and properties, frequency-dependent moments, and moderately accurate excitation energies. In a sense these properties have all been calculated simultaneously.

The general purpose of this paper is to study the functional form of Σ given in STY (upon which the calculation of Yarlagadda *et al.*[1] is based). (Throughout this work we are implicitly assuming that the functional form of the STY optical potential is more correct than the GRPA method that is used in the calculation.) This functional form consists of three terms [Eqs. (4.6) and (4.11a) of STY]: the Hartree-Fock term, the direct polarization term [containing the two-point response function $R(32, 3^+2^+)$], and the exchange polarization term [containing the three-point response function $R(32, 1'^+2^+)$]. In particular we shall seek (i) ways of using semiempirical data (on frequency-dependent moments and adsorption coefficients) in constructing Σ, and from Σ, the aforementioned properties; (ii) alternate methods of computing Σ using the excellent variation-perturbation methods of Karplus and Kolker,[3] Yaris,[4,5] and Dalgarno and Epstein[6]; (iii) to demonstrate and interpret the relation of this Σ to the multitude of optical potentials used in elastic electron-atom, -molecule scattering calculations, in the determination of Rydberg states of atoms (molecules), and for the core pseudopotentials in solids (Bethe,[7] Temkin,[8] Mittleman and Watson,[9] Lippman *et al.*,[10] LaBahn and Callaway,[11,12] Khare and Shobha,[13] Kestner